

Spin-gap formation due to spin-Peierls instability in π -orbital-ordered NaO_2

Mizuki Miyajima,^{1,*} Fahmi Astuti^{2,3,*}, Takahito Fukuda,¹ Masashi Kodani,¹ Shinsuke Iida,⁴ Shinichiro Asai,⁴ Akira Matsuo,⁴ Takatsugu Masuda,^{4,5,6} Koichi Kindo,⁴ Takumi Hasegawa,⁷ Tatsuo C. Kobayashi,¹ Takehito Nakano,⁸ Isao Watanabe,^{2,3} and Takashi Kambe^{1,§}

¹Department of Physics, Okayama University, Okayama 700-8530, Japan

²Advanced Meson Science Laboratory, RIKEN Nishina Center, Wako, Saitama 351-0198, Japan

³Department of Physics, Hokkaido University, Sapporo 060-0808, Japan

⁴Institute for Solid State Physics, University of Tokyo, Kashiwa, Chiba 277-8581, Japan

⁵Institute of Materials Structure Science, High Energy Accelerator Research Organization, Tsukuba, Ibaraki 305-0801, Japan

⁶Trans-scale Quantum Science Institute, University of Tokyo, Tokyo 113-0033, Japan

⁷Graduate School of Advanced Science and Engineering, Hiroshima University, Higashi-Hiroshima, 739-8521, Japan

⁸Institute of Quantum Beam Science, Ibaraki University, Mito, Ibaraki 310-8512, Japan

 (Received 19 June 2021; revised 16 August 2021; accepted 23 September 2021; published 7 October 2021)

We have investigated the low-temperature magnetism of sodium superoxide (NaO_2), in which spin, orbital, and lattice degrees of freedom are closely entangled. The magnetic susceptibility shows anomalies at $T_1 = 220$ K and $T_2 = 190$ K, which correspond well to the structural phase transition temperatures, and a sudden decrease below $T_3 = 34$ K. At 4.2 K, the magnetization shows a clear stepwise anomaly around 30 T with a large hysteresis. In addition, the muon spin relaxation experiments indicate no magnetic phase transition down to $T = 0.3$ K. The inelastic neutron scattering spectrum exhibits magnetic excitation with a finite energy gap. These results confirm that the ground state of NaO_2 is a spin-singlet state. To understand this ground state in NaO_2 , we performed Raman scattering experiments. All the Raman-active libration modes expected for the marcasite phase below T_2 are observed. Furthermore, we find that several new peaks appear below T_3 . This directly evidences the low crystal symmetry, namely, the presence of the phase transition at T_3 . We conclude that the singlet ground state of NaO_2 is due to the spin-Peierls instability.

DOI: [10.1103/PhysRevB.104.L140402](https://doi.org/10.1103/PhysRevB.104.L140402)

The entanglement of spins, orbitals, charge, and lattice degrees of freedom is a fundamental issue in solid-state physics [1–4]. They yield a variety of phenomena such as superconductivity, quantum liquids, multiferroics, and orbital liquids [5–7]. While these physics have been discussed mainly in d - and f -electron systems, there has been very little discussion in p - or π -electron systems [8,9]. The magnetism of alkali-metal superoxide, AO_2 , originates from the unpaired p electrons on the O_2 molecule. In O_2 , as two unpaired electrons occupy two π_g^* orbitals, π_x^* and π_y^* , whose spins are in parallel to each other, O_2 is a magnetic molecule with the spin quantum number, S , of 1. In AO_2 , as the A cation is usually fully ionized, the additional electron on O_2 occupies one of two half-filled π_g^* orbitals. This allows the O_2^- molecule to gain the orbital degrees of freedom. As three electrons exist on two π_g^* 's, the energy band for the O_2^- state is quarter filled. The *ab initio* band calculations for AO_2 show that the Fermi energy locates within the π band [10–12]. On the contrary, the experimental magnetic properties suggest electron localization,

which implies the importance of an electronic correlation on the O_2 molecule. Thus, AO_2 should be considered as a Mott insulator [10,11]. Magnetoelastic coupling should occur to lift the degeneracy of the π_g^* orbital, which leads to the selection of the π^* orbitals. The coherent arrangement of the O_2 orbitals is expected to lead to a three-dimensional magnetic exchange interaction between the spins. Therefore, in AO_2 , spins, orbitals, charge, and lattice degrees of freedom are strongly coupled [12]. AO_2 is expected to be a candidate material to exhibit such fascinating phenomena.

Recently, AO_2 has attracted much attention for its magnetic quantum phenomena at low temperatures [13–19]. CsO_2 shows one-dimensional (1D) antiferromagnetic (AFM) behavior in the magnetic susceptibility and the high magnetic field magnetization [13,16]. It was suggested that a 1D chain should form as a result of the π -orbital ordering, but the detailed low-temperature structure has not been determined [13]. NMR experiments showed a power-law dependence of the spin-lattice relaxation function, suggesting the emergence of a Tomonaga-Luttinger liquid state in the 1D short-range-ordered phase [14].

Contrary to RbO_2 and CsO_2 , NaO_2 has a cubic (space group: $Fm\bar{3}m$) symmetry at room temperature, in which O_2 has an orientational disorder [20]. With decreasing temperature, NaO_2 shows successive structural phase transitions at $T_1 = 220$ and $T_2 \sim 196$ K [20]. In the marcasite phase below

*These authors contributed equally to this work.

†Present address: Institute for Molecular Science, Okazaki, Japan.

‡Present address: Department of Physics, Institut Teknologi Sepuluh Nopember, Indonesia.

§Corresponding author: kambe@science.okayama-u.ac.jp

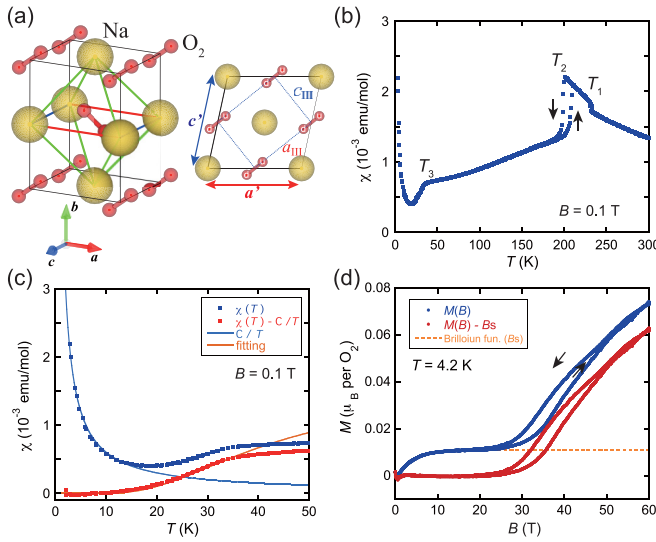


FIG. 1. (a) Unit cell of the marcasite phase of NaO_2 . The right figure shows the unit cell in the ac plane. a_{III} and c_{III} denote the axes in the phase III while a' and c' correspond to that in the phase II. (b) Temperature dependence of magnetic susceptibility, $\chi(T)$, at $B = 0.1$ T in powder NaO_2 . $\chi(T)$ shows clear anomaly at T_1 , T_2 , and T_3 . The arrows indicate the hysteresis in the cooling and heating protocols. (c) Enlarged figure around T_3 . The experimental data $\chi(T)$ (blue dot), the low-temperature Curie tail C_0/T (blue line), and the subtracted data $\chi(T) - C_0/T$ (red dot) are shown. $\chi(T)$ is fitted by the equation in the text. (d) High magnetic field magnetization at 4.2 K, where the vertical axis indicates the magnetization per O_2 . At low magnetic field region, the $M(B)$ curve can be fitted by the Brillouin function, B_s . The experimental data $M(B)$ (blue dot), the B_s (orange dotted line), and the subtracted data $M(B) - B_s$ (red dot) are shown.

T_2 , the degeneracy of the π_g^* orbitals is considered to be lifted due to the low local symmetry around O_2 . The magnetic susceptibility shows a weak decrease below T_2 and, then, a sudden drop below $T_3 = 30 \sim 40$ K. These experimental findings remind us of the low dimensionality of the spin system and of a magnetic phase change below T_3 . Theoretical calculations for the marcasite phase pointed to the quasi-1D AFM character along the c axis and frustration of exchange interactions between different sublattice spins [21]. However, because of no experimental inspection on the existence of the magnetic phase transition and a change in crystal symmetry, the magnetic ground state of NaO_2 has not yet been clarified. In this Letter, we investigate low-temperature magnetic and structural properties of the π -orbital system NaO_2 in detail. For this purpose, we performed magnetic susceptibility, high-field magnetization, muon spin relaxation (μSR), x-ray diffraction (XRD), inelastic neutron scattering (INS), and Raman scattering experiments using high-quality samples.

First, we define three phases [20]: phase I above T_1 , phase II between T_1 and T_2 , and phase III between T_2 and T_3 . NaO_2 has a remarkable temperature dependence of magnetic susceptibility, $\chi = M/B$, where M and B denote the magnetization and the magnetic field, respectively. Figure 1(b) shows the temperature dependence of $\chi(T)$ for a powder sample using a cooling and heating protocol with a magnetic field of 0.1 T.

$\chi(T)$ shows anomalies around T_1 , T_2 , and T_3 , which is consistent with the literature [22]. The temperatures of T_1 and T_2 correspond well to the structural phase transition temperatures [23]. In phase I, the $\chi(T)$ follows the Curie-Weiss law with a negative Weiss constant of $\theta = -9.4$ K. Small θ indicates a weak AFM interaction, which should be due to the orientational disorder of O_2 . In phase II, the θ changes to 41.1 K, suggesting ferromagnetic correlations due to the orientational ordering of O_2 . The effective magnetic moments above and below T_1 are estimated to be about 1.82 and 1.68 μ_B , respectively, which increase slightly from the value expected from the spin only. This may be due to the orbital effect. Following a clear hysteresis around T_2 , which indicates a first-order phase transition, $\chi(T)$ shows a weak decrease with decreasing temperature. As the localized spins on O_2 are responsible for the magnetism of NaO_2 , the remarkable decrease of $\chi(T)$ in the phase III is an important key to consider the low-temperature magnetism [21,24]. In other words, it may be reasonable to think that it comes from low-dimensionality. To evaluate J from the $\chi(T)$, we used the Bonner-Fisher model [25] and a two-dimensional model with weak interchain interaction [26], as shown in Fig. S3 in the Supplemental Material [23]. However, we could not reproduce the experiments by these models using the temperature-independent J . The XRD experiments showed that the thermal shrinkage coefficient of the c axis was -5.16×10^{-4} ($\text{\AA}/\text{K}$), which was the largest value among the principal axes. Thus, the shrinkage of the nearest-neighbor (NN) length between O_2 's, which corresponds to the c -axis length, may be sufficient to make AFM J stronger as the temperature decreases.

Below T_3 , $\chi(T)$ decreases rapidly with decreasing temperature with no temperature hysteresis and, then, increases. The μSR experiment showed that no magnetic ordering was found down to 0.3 K as described later. Therefore, the decrease of $\chi(T)$ implies the appearance of a spin gap in the spin excitation spectrum. Note that the low-temperature Curie tail is strongly dependent on the sample batch, indicating that it is due to the extrinsic spins. To evaluate the intrinsic temperature dependence of $\chi(T)$, we use the equation $\chi(T) = C_0/T + C/T \exp(-2\Delta/k_B T)$, where the Δ denotes the spin gap and k_B is the Boltzmann constant [27,28]. The first term is the Curie-tail contribution, which can be subtracted from the data, and the second term is responsible for the spins excited from the singlet state to the magnetic excited states. As shown in Fig. 1(c), the fitting by this equation with $\Delta/k_B = 51.2$ K is good. The Curie tail allows us to estimate the number of extrinsic spins with $S = 1/2$ to be 0.014 mol in this sample.

Figure 1(d) shows the magnetization curve, $M(B)$, as a function of B up to 60 T at $T = 4.2$ K. The saturation magnetization is equivalent to $\sim 1 \mu_B$. Note that the $M(B)$ experiment was performed using the same sample as the $\chi(T)$ experiments. At $T = 4.2$ K, the $M(B)$ shows a nonlinear increase at low fields and an anomaly with a large hysteresis around ~ 30 T. To evaluate the low magnetic field part of the $M(B)$ curve, we use a Brillouin function as shown in Fig. 1(d). The fitting was good and the number of paramagnetic spins was obtained to be 0.011 mol. This value is consistent with that obtained from the Curie tail in the $\chi(T)$ experiment, allowing us to subtract the low-field Brillouin contribution from the $M(B)$ curve. Accordingly, $M(B)$ shows the magnetic-field-induced

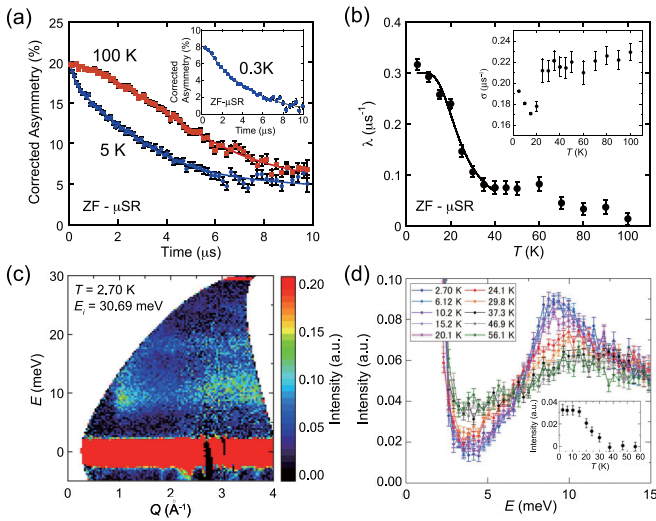


FIG. 2. (a) Zero-field (ZF) μ SR spectra of NaO_2 at 5 K and 100 K. The inset shows ZF μ SR spectrum at 0.3 K. The solid lines are the fitted curves using the equation in the text. (b) Temperature dependence of λ . The solid line is the fitted curve using the gap-related analysis function described in the text [27,28]. The inset shows the temperature dependence of σ . (c) INS spectra after background subtraction. Details are described in the Supplemental Material [23]. (d) INS profiles, where the spectra between 0.5 \AA^{-1} and 1.5 \AA^{-1} are integrated. Temperature dependence of the intensity at 9.4 meV is shown in the inset.

transition from nonmagnetic to magnetic state with the large hysteresis around $\sim 30 \text{ T}$.

To find out any signatures of a magnetic ordering in NaO_2 , we performed μ SR experiments down to 0.3 K . Figure 2(a) shows corrected time spectra measured at 0.3 K ($\ll T_3$), 5 K , and 100 K ($\gg T_3$) in the zero-field (ZF) condition. Neither the loss of the initial asymmetry at $t = 0$ nor the muon-spin precession was observed down to 0.3 K . These findings exclude the presence of a long-range magnetic order down to 0.3 K .

To focus on collecting some data points around T_3 , we analyzed the depolarization rate obtained in ZF by using the function: $A(t) = Ae^{-\lambda t} e^{-(\sigma t)^2} + BG$ [29]. Here, the Gaussian term arises from the muon-spin relaxation caused by randomly distributed internal fields coming from surrounding nuclear dipoles. The exponential term describes the effect of the fluctuating electronic moments around the muon [30,31]. The BG indicates background signals from muons which do not stop in the sample but in a sample mounting plate. These BG signals were subtracted from the raw signal as a constant term in order to achieve corrected μ SR time spectra.

The temperature dependencies of λ and σ are shown in Fig. 2(b). Above T_3 , we obtained $\lambda \sim 0.1$ and $\sigma \sim 0.22 \mu\text{s}^{-1}$. The result of λ obtained above T_3 indicates that electronic spins likely fluctuate beyond the μ SR characteristic time window ($10^{-6} \sim 10^{-11} \text{ sec}$), resulting in the motional narrowing limit. The λ increase below T_3 suggests that the muon is expected to sense the formation of the spin-gap state in NaO_2 . One possible scenario to explain this result is that the muon spin relaxes its polarization by the thermally activated electronic spins across the spin gap. The same behavior was observed in other spin-gap systems [27].

Following this scenario, the spin gap is estimated from the temperature dependence of λ below T_3 by applying the following function: $\lambda(T) = \lambda_0 \{1 + C' \exp(-2\Delta/k_B T)\}^{-1}$ [27,28]. Using this equation, we estimated the Δ/k_B to be $\sim 44.6 \text{ K}$, which was consistent with that obtained from the magnetic susceptibility measurement.

Figure 2(c) shows the INS spectra of the powder sample at 2.70 K , where the background contribution was subtracted (see Supplemental Material [23]). The excitation around $Q \sim 1 \text{ \AA}^{-1}$ is shown to have a finite energy gap. The intensity decreases with Q , which is typical behavior of magnetic scattering, in the range of $Q \lesssim 2 \text{ \AA}^{-1}$. The enhanced intensity at $Q \gtrsim 2 \text{ \AA}^{-1}$ is from remnant phonon scattering of the sample cell made of aluminum. The first momentum of the dynamical structure factor in the 1D AFM spin chain is proportional to $1 - \sin Qd/Qd$, where d is the distance between spins [32], leading to the pronounced intensity at $Q \sim 1 \text{ \AA}^{-1}$.

To reveal the change in the intensity as a function of temperature, the spectra integrated between 0.5 \AA^{-1} and 1.5 \AA^{-1} are shown in Fig. 2(d). At 2.70 K , the intensity starts to increase at $E \sim 4 \text{ meV}$ and has a maximum at $E \sim 9 \text{ meV}$. The temperature dependence of the intensity at the maximum energy is shown in the inset. It shows no temperature dependence above T_3 , and gradually increases with decreasing temperature below T_3 . This result directly indicates that NaO_2 has the magnetic excitation with an excitation gap energy of 9 meV below T_3 . As the μ SR experiments indicated no magnetic long-range ordering down to 0.3 K , this peak results not from magnetic excitation in the magnetic long-range-ordered phase but from singlet-triplet excitation in the nonmagnetic ground state.

We searched for structural dimerization of the O_2 molecules as the cause of the nonmagnetic state by the XRD and neutron diffraction measurements, but could not experience the direct evidence on the structural change below T_3 [23]. Then, we perform Raman scattering experiments because of high sensitivity to changes in crystal symmetry and/or molecular charge. Figures 3(a) and 3(b) show the temperature dependence of the Raman scattering spectra in the stretching and the libration mode region of O_2 , respectively. We will focus on the change of the Raman-active modes around T_3 .

As the crystal symmetry of phase III is determined as $Pnmm$ (D_{2h}), the sets of Raman active stretching and libration modes are given by $\Gamma_S = A_g + B_{1g}$ and $\Gamma_L = B_{1g} + B_{3g} + A_g + B_{2g}$, respectively [33,34]. As shown in Fig. 3(a), two peaks can be clearly observed in the stretching mode region. We can assign that the peaks at 1163 cm^{-1} and 1140 cm^{-1} originate from the in-phase and the out-of-phase stretching modes, namely, A_g and B_{1g} , respectively. In the libration mode region [see Fig. 3(b)], two major peaks are observed around 150 cm^{-1} (L_3) and 240 cm^{-1} (L_1), and very weak peaks are observed around 130 cm^{-1} (L_4) and 190 cm^{-1} (L_2). Note that these peaks were not observed at room temperature, and appeared below T_2 , indicating that they do not originate from impurities, but are intrinsic signals of NaO_2 . The libration modes can be assigned from the intensity and energy, but a more detailed consideration will be needed. Anyway, these results demonstrate that all Raman active modes for the phase with the D_{2h} symmetry can be successfully detected [33]. Below

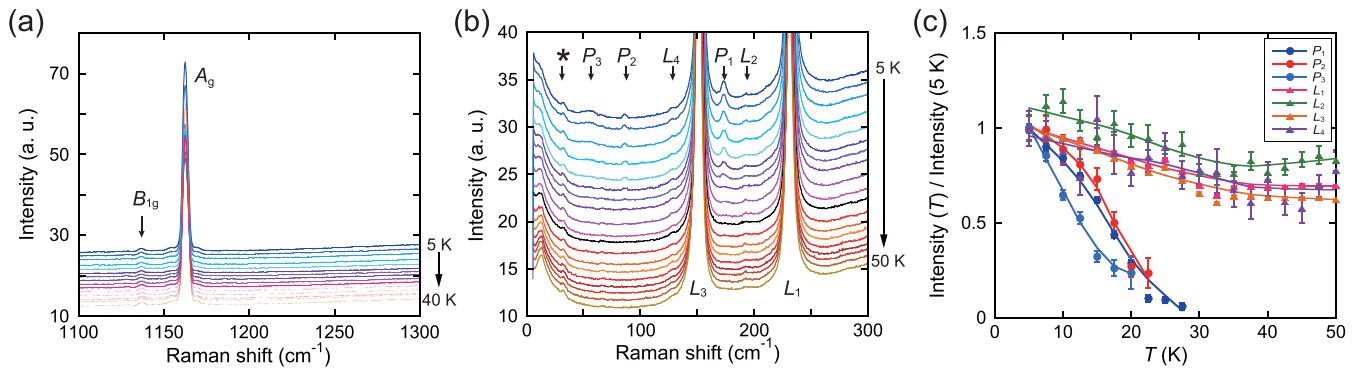


FIG. 3. Raman scattering results of NaO₂. (a) and (b): Temperature dependencies of the stretching modes and the libration modes below 50 K, respectively. The spectra are shifted along the vertical axis for clarity. The asterisk peak is a line included in the laser source. (c) Temperature dependencies of peak intensity for the libration mode region, where the peak intensities are normalized by the intensity at 5 K. At low temperatures, these peak intensities might not be saturated due to laser heating. Solid lines are guides to the eye.

T_3 , while no change was observed in the stretching mode region, in the libration mode region, new peaks at 173, 86, and 56 cm⁻¹ gradually appeared, which are represented as P_1 , P_2 , and P_3 in Fig. 3(b), respectively. Figure 3(c) summarizes the temperature dependence of the peak intensity observed in the libration mode region. While the Γ_L modes depended weakly on the temperatures, the P_1 , P_2 , and P_3 peak intensities increased markedly below 30 K, following order-parameter-like behavior. Note that no splittings of the stretching modes are found, suggesting an absence of charge ordering on O₂. Thus, this result clearly indicates an existence of a phase transition around T_3 . Because all Raman-active Γ_L modes are confirmed in phase III, the observation of the new peaks is direct evidence of the low crystal symmetry below T_3 .

To discuss the cause of the nonmagnetic state, it is necessary to understand the crystal structure of the precursor phase, i.e., the phase III. O₂ is octahedrally surrounded by Na atoms in all phases. In phase II, the molecular axis is aligned along one of the four equivalent [111] directions of the octahedron (see Supplemental Material [23]). The NN molecules arrange their molecular axes to avoid each other, i.e., coherent *antiferro*-like arrangement of the molecular axes. Because the symmetry of the octahedron is still cubic, the degeneracy of the π_g^* orbital should be conserved. On the contrary, in phase III, the threefold symmetry of the octahedron is lost and the molecular axis is slightly tilted from the [111] direction of the octahedron. Na-Na bond lengths are changed to be not equivalent and the Na-O bond length is increased along the b axis. [In Fig. 1(a), different Na-Na bond lengths are displayed by colors.] The NN molecules within the ac plane arrange their molecular axes to be parallel to each other; namely, the *ferro*-like arrangement of the molecular axes is realized. Thus, the NN molecular axes are parallel to each other along the c axis while they are canted along the a and b axes. The twofold distortion of the octahedron should break the orbital degeneracy, and stabilizes the π_g^* orbital perpendicular to the c axis as the unoccupied orbital. Namely, a *ferro*-orbital ordering is realized in the ac plane. The c -axis length, i.e., the length between the NN molecules, is obtained to be 3.39 Å at 100 K, which is close to the length between molecules in the α phase of the solid O₂ (~ 3.2 Å) [35,36]. Consequently, we can expect the strong AFM exchange interaction along the c axis. This

structural peculiarity should be manifested in the $\chi(T)$ below T_2 , namely, the low-dimensional nature. Moreover, because there was no structural dimerization of O₂ in any directions in all phases, we were able to deny both isolated dimerization of O₂ and 1D alternating AFM chain as the cause of the spin gap. Accordingly, we can conclude that the magnetism in phase III is based on the uniform AFM spin chain and, then, the magnetic ground state is the spin-Peierls (SP) state.

Finally, we consider the SP state in NaO₂. As the spin-gap value and the SP transition temperature are obtained to be $\Delta/k_B = 51.2$ K and $T_3 = T_{SP} = 34$ K, respectively, from the magnetic measurements, the value of $2\Delta/k_B T_{SP}$ is calculated to be 3.01. This is comparable with the BCS weak-coupling result (3.54). The alternating exchange interaction constants, J_1 and J_2 , in the SP state can be written as $J_{1,2} = J(1 \pm \delta)$ using the alternating parameter δ [37]. The spin gap is also related to $\Delta = 2pJ\delta$ with $p \sim 1 + 2/\pi$. Using Bulaevskii's formula for the $\chi(T)$ below the SP transition [38], we estimate the δ by fitting to the experiment. When we use the $J/k_B = 140$ K in the 1D uniform AFM phase, which was obtained around 50 K, we obtain the δ of 0.11. For the organic SP compounds TTF-CuBDT [39] and the inorganic CuGeO₃ [40], the δ was estimated to be 0.167 and 0.167, respectively. The δ in NaO₂ is comparable to these values. Moreover, the δ of 0.11 roughly leads to the Δ/k_B of 51 K, which is almost identical to the spin-gap value obtained in the experiment. It is known that the AFM J of the solid-O₂ magnet depends exponentially on the intermolecular length [36,41–43]. As we expect that the direct magnetic interaction between NN O₂'s along the c axis is dominant, the same dependence can be applied. If so, even though the lattice dimerization in NaO₂ would be extremely small and not observed experimentally, the J alternation may occur in the SP phase. More detailed structural study in the SP phase of NaO₂ is a future task.

In summary, we have investigated the low-temperature magnetism of NaO₂. We found no magnetic phase transition down to $T = 0.3$ K and confirmed the spin-singlet ground state below T_3 . Raman scattering experiments clearly indicated the presence of the phase transition at T_3 . Consequently, we conclude that the singlet ground state of NaO₂ is due to the SP instability.

The authors acknowledge fruitful discussions with H. O. Jeschke, J. Otsuki, M. Naka, K. Okada, R. Kondo, T. Goto, H. Sagayama, and R. Kumai. The x-ray diffraction study was performed under the approval of the Photon Factory Program Advisory Committee (Proposals No. 2017G636, No. 2019T003, and No. 2020G666). The neu-

tron scattering experiment at the HRC was approved by the Neutron Scattering Program Advisory Committee of IMSS, KEK (Proposal No. 2019S01), and ISSP. This work was partly supported by JSPS KAKENHI (Grants No. 15H03529, No. 20K20896, and No. 21H04441), MEXT, Japan.

- [1] Y. Tokura and N. Nagaosa, *Science* **288**, 462 (2000).
- [2] J. B. Goodenough, *Magnetism and the Chemical Bond* (Wiley Interscience, New York, 1963).
- [3] K. I. Kugel and D. I. Khomskii, *Sov. Phys. Usp.* **25**, 231 (1982).
- [4] J. Kanamori, *J. Phys. Chem. Solids* **10**, 87 (1959).
- [5] Y. Ishiguro, K. Kimura, S. Nakatsuji, S. Tsutsui, A. Q. R. Baron, T. Kimura, and Y. Wakabayashi, *Nat. Commun.* **4**, 2022 (2013).
- [6] T. Kimura, T. Goto, H. Shintani, K. Ishizaka, and T. Arima, and Y. Tokura, *Nature (London)* **426**, 55 (2003).
- [7] S. Ishihara, M. Yamanaka, and N. Nagaosa, *Phys. Rev. B* **56**, 686 (1997).
- [8] S. Margadonna, K. Prassides, H. Shimoda, T. Takenobu, and Y. Iwasa, *Phys. Rev. B* **64**, 132414 (2001).
- [9] T. Kambe, K. Kajiyoshi, M. Fujiwara, and K. Oshima, *Phys. Rev. Lett.* **99**, 177205 (2007).
- [10] M. Kim and B. I. Min, *Phys. Rev. B* **89**, 121106(R) (2014).
- [11] R. Kováčik, P. Werner, K. Dymkowski, and C. Ederer, *Phys. Rev. B* **86**, 075130 (2012).
- [12] I. V. Solovyev, *New J. Phys.* **10**, 013035 (2008).
- [13] S. Riyadi, B. Zhang, R. A. de Groot, A. Caretta, P. H. M. van Loosdrecht, T. T. M. Palstra, and G. R. Blake, *Phys. Rev. Lett.* **108**, 217206 (2012).
- [14] M. Klanjšek, D. Arčon, A. Sans, P. Adler, M. Jansen, and C. Felser, *Phys. Rev. Lett.* **115**, 057205 (2015).
- [15] T. Knaflič, M. Klanjšek, A. Sans, P. Adler, M. Jansen, C. Felser, and D. Arčon, *Phys. Rev. B* **91**, 174419 (2015).
- [16] M. Miyajima, F. Astuti, T. Kakuto, A. Matsuo, D. P. Sari, R. Asih, K. Okunishi, T. Nakano, Y. Nozue, K. Kindo, I. Watanabe, and T. Kambe, *J. Phys. Soc. Jpn.* **87**, 063704 (2018).
- [17] F. Astuti, M. Miyajima, T. Fukuda, M. Kodani, T. Nakano, T. Kambe, and I. Watanabe, *J. Phys. Soc. Jpn.* **88**, 043701 (2019).
- [18] Fahmi Astuti, Ph.D. thesis, Hokkaido University, 2019.
- [19] Mizuki Miyajima, Ph.D. thesis, Okayama University, 2021.
- [20] M. Ziegler, M. Rosenfeld, and W. Känzig, *Helv. Phys. Acta* **49**, 57 (1976).
- [21] I. V. Solovyev, Z. V. Pchelkina, and V. V. Mazurenko, *Crypt. Eng. Commun.* **16**, 522 (2014).
- [22] A. Zumsteg, M. Ziegler, W. Känzig, and M. Bösch, *J. Phys.: Condens. Matter* **17**, 267 (1974).
- [23] See Supplemental Material at <http://link.aps.org/supplemental/10.1103/PhysRevB.104.L140402> where the crystal structures for the phases are analyzed by the Rietveld refinement and are shown. We also estimate the upper limit of a distortion along the c axis, where the strong AFM interaction should be present between the NN O₂'s, by taking into account the systematic error of the experimental background in the neutron elastic diffraction experiments.
- [24] S. D. Mahanti and G. Kemeny, *Phys. Rev. B* **20**, 2105 (1979).
- [25] J. C. Bonner and M. E. Fisher, *Phys. Rev.* **135**, A640 (1964).
- [26] B. C. Keith, C. P. Landee, T. Valteau, M. M. Turnbull, and N. Harrison, *Phys. Rev. B* **84**, 104442 (2011).
- [27] P. J. Baker, S. J. Blundell, F. L. Pratt, T. Lancaster, M. L. Brooks, W. Hayes, M. Isobe, Y. Ueda, M. Hoinkis, M. Sing, M. Klemm, S. Horn, and R. Claessen, *Phys. Rev. B* **75**, 094404 (2007).
- [28] E. Ehrenfreund and L. S. Smith, *Phys. Rev. B* **16**, 1870 (1977).
- [29] R. S. Hayano, Y. J. Uemura, J. Imazato, N. Nishida, T. Yamazaki, and R. Kubo, *Phys. Rev. B* **20**, 850 (1979).
- [30] I. Watanabe, M. Akoshima, Y. Koike, S. Ohira, and K. Nagamine, *Phys. Rev. B* **62**, 14524 (2000).
- [31] T. Adachi, N. Oki, Risdiana, S. Yairi, Y. Koike, and I. Watanabe, *Phys. Rev. B* **78**, 134515 (2008).
- [32] I. Zaliznyak and S. Lee, *Magnetic Neutron Scattering in Modern Techniques for Characterizing Magnetic Materials*, edited by Y. Zhu (Springer, Heidelberg, 2005).
- [33] J. B. Bates, M. H. Brooker, and G. E. Boyd, *Chem. Phys. Lett.* **16**, 391 (1972).
- [34] M. Bösch and W. Känzig, *Helv. Phys. Acta* **48**, 743 (1975).
- [35] G. C. DeFotis, *Phys. Rev. B* **23**, 4714 (1981).
- [36] C. Uyeda, K. Sugiyama, and M. Date, *J. Phys. Soc. Jpn.* **54**, 1107 (1985).
- [37] E. Pytte, *Phys. Rev. B* **10**, 4637 (1974).
- [38] N. Bulaevskii, *Fiz. Tverd. Tela (Leningrad)* **11**, 1132 (1969).
- [39] J. W. Bray, H. R. Hart, L. V. Interrante, I. S. Jacobs, J. S. Kasper, G. D. Watkins, S. H. Wee, and J. C. Bonner, *Phys. Rev. Lett.* **35**, 744 (1975).
- [40] M. Hase, I. Terasaki, and K. Uchinokura, *Phys. Rev. Lett.* **70**, 3651 (1993).
- [41] M. C. van Hemert, P. E. S. Wormer, and A. van der Avoird, *Phys. Rev. Lett.* **51**, 1167 (1983).
- [42] Paul E. S. Wormer and Ad van der Avoird, *J. Chem. Phys.* **81**, 1929 (1984).
- [43] B. Bussery, S. Ya. Umanskii, M. Aubert-Frécon, and O. Bouty, *J. Chem. Phys.* **101**, 416 (1994).